Influence of Cholesterol and β-Sitosterol on the Structure of EYPC Bilayers

Gallová, Jana; Uhrıková, Daniela; Kučerka, Norbert; Svorková, Miroslava; Funari, Sergio S.; Murugova, Tatiana N.; Almásy, László; Mazúr, Milan; Balgavý, Pavol

Publisher's version / Version de l'éditeur:
https://doi.org/10.1007/s00232-011-9387-1
The Journal of Membrane Biology, 243, 1-3, pp. 1-13, 2011-08-04

J Membrane Biol (2011) 243:1–13
DOI 10.1007/s00232-011-9387-1

ORIGINAL ARTICLES

Influence of Cholesterol and β-Sitosterol on the Structure of EYPC Bilayers

Jana Gallová · Daniela Uhríková · Norbert Kučerka · Miroslava Svorková · Sergio S. Funari · Tatiana N. Murugova · László Almásy · Milan Mazúr · Pavol Balgavý

Received: 14 September 2010 / Accepted: 13 July 2011 / Published online: 4 August 2011

Abstract The influence of cholesterol and β-sitosterol on egg yolk phosphatidylcholine (EYPC) bilayers is compared. Different interactions of these sterols with EYPC bilayers were observed using X-ray diffraction. Cholesterol was miscible with EYPC in the studied concentration range (0–50 mol%), but crystallization of β-sitosterol in EYPC bilayers was observed at $X \geq 41$ mol% as detected by X-ray diffraction. Moreover, the repeat distance (d) of the lamellar phase was similar upon addition of the two sterols up to mole fraction 17%, while for $X \geq 17$ mol% it became higher in the presence of β-sitosterol compared to cholesterol. SANS data on suspensions of unilamellar vesicles showed that both cholesterol and β-sitosterol similarly increase the EYPC bilayer thickness. Cholesterol in amounts above 33 mol% decreased the interlamellar water layer thickness, probably due to "stiffening" of the bilayer. This effect was not manifested by β-sitosterol, in particular due to the lower solubility of β-sitosterol in EYPC bilayers. Applying the formalism of partial molecular areas, it is shown that the condensing effect of both sterols on the EYPC area at the lipid–water interface is small, if any. The parameters of ESR spectra of spin labels localized in different regions of the EYPC bilayer did not reveal any differences between the effects of cholesterol and β-sitosterol in the range of full miscibility.

Keywords Cholesterol · β-Sitosterol · Plant sterol · Egg yolk phosphatidylcholine · Repeat distance · Bilayer thickness · Undulation · SANS · X-ray diffraction · ESR

J. Gallová (✉) · D. Uhríková · N. Kučerka · M. Svorková · P. Balgavý
Department of Physical Chemistry of Drugs, Faculty of Pharmacy, Comenius University, Odbojárov 10, 832 32 Bratislava, Slovakia
e-mail: gallova@fpharm.uniba.sk

N. Kučerka
Canadian Neutron Beam Centre, National Research Council, Chalk River, ON K0J 1P0, Canada

S. S. Funari
HASYLAB at DESY, 22603 Hamburg, Germany

T. N. Murugova
Frank Laboratory of Neutron Physics, Joint Institute for Nuclear Research, 141980 Dubna, Russia

L. Almásy
Laboratory for Neutron Scattering, PSI, 5232 Villigen, Switzerland

L. Almásy
Research Institute for Solid State Physics and Optics, POB 49, Budapest 1525, Hungary

M. Mazúr
Faculty of Chemical and Food Technology, Institute of Physical Chemistry and Chemical Physics, Slovak University of Technology, 81237 Bratislava, Slovakia

Introduction

Sterols are essential membrane components in eukaryotes. While mammalian cells contain almost exclusively only one sterol, namely cholesterol, plant membranes contain a mixture of sterols including such major representatives like β-sitosterol, campesterol and stigmasterol. Recently, plant sterols (phytosterols) have attracted much attention because of their capability to reduce cholesterol absorption in the intestine and, hence, to protect against cardiovascular diseases (Plat and Mensink 2005). Moreover, β-sitosterol has also antiseptic, antineoplastic and antipyretic effects (Ovesná et al. 2004). Epidemiological and experimental

studies have indicated that plant sterols may provide protection against cancers of the colon, breast and prostate (Awad and Fink 2000). On the other hand, some negative effects have been observed for parenteral administration of plant sterols to laboratory animals (Ling and Jones 1995). In particular, β-sitosterol at high plasma concentrations may have cytotoxic effects. Therefore, it is interesting to examine the difference between the cholesterol and β-sitosterol interactions with the lipid bilayer as a model of biological membranes. The structures of cholesterol (Fig. 1a) and β-sitosterol (Fig. 1b) differ only in an ethyl substituent on C24 in the side chain.

Several authors have studied the interaction of β-sitosterol with synthetic phosphatidylcholines with saturated chains (Bernsdorff and Winter 2003; Halling and Slotte 2004; Su et al. 2007; Gao et al. 2008). In the present study, we compared the influence of cholesterol and β-sitosterol on the natural lipid phosphatidylcholine isolated from egg yolk (EYPC). Gas chromatographic analysis showed that EYPC contains 43% residues of saturated fatty acids, of which palmitic acid (C16:0) represents 30% and stearic acid (C18:0) 12%. The major residues of unsaturated fatty acids were represented by oleic acid (C18:1) 28%, linoleic acid (C18:2) 14%, arachidonic acid (C20:4) 4%, docosapentaeonic acid (C22:5) 2% and docosahexaenoic acid (C22:6) 4.4% (Filípek et al. 1993). Natural phospholipids usually have one unsaturated acyl chain in the *sn*-2 position (Hauser and Poupart 2009). EYPC bilayers in multilamellar liposomes at temperatures above 0°C are in a disordered fluid (L_d) state. The phase diagrams of EYPC + cholesterol and EYPC + β-sitosterol systems have not been systematically investigated yet. However, several authors have studied 1-palmitoyl-2-oleoyl phosphatidylcholine (POPC), which is a major component of EYPC. POPC in the presence of approximately 30 mol% cholesterol occurs in a liquid ordered (L_o) phase (Thewalt and Bloom 1992). A study of POPC bilayers at 25°C identified the coexistence of L_d and L_o phases in the range 10–40 mol% cholesterol, while above 40 mol% cholesterol only the L_o phase was observed (Mateo et al. 1995; de Almeida et al. 2003). A gradual transition from L_d to L_o phase without any coexistence range was observed by fluorescence microscopy (Veatch and Keller 2005). Hence, it follows that any L_o and L_d domains observed by other methods are smaller than 1 μm. With respect to the composition of acyl chains in EYPC (Filípek et al. 1993), we suppose that EYPC behaves in a similar manner as POPC; i.e., with increasing concentrations of cholesterol the L_d state of the EYPC bilayer transforms to L_o gradually or through coexistence of L_d and L_o.

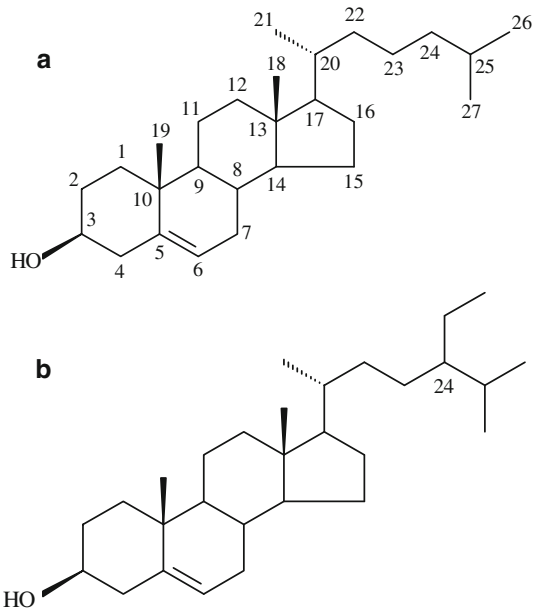

Fig. 1 **a** Structure of cholesterol. **b** Structure of ß-sitosterol

Materials and Methods

Chemicals

Phosphatidylcholine from hen egg yolks (EYPC) was isolated and purified according to Singleton et al. (1965). Cholesterol and β-sitosterol were purchased from Sigma-Aldrich (Taufkirchen, Germany). Spin labels 2-(14-carboxytetradecyl)-2-ethyl-4,4-dimethyl-3-oxazolidinyloxy (16-DSA) was from Sigma-Aldrich, 3-spiro-[2′-(*N*-oxyl-4′,4′-dimethyloxazolidine)] derivative of 5a-cholestan-3-one (CSL) was obtained from Syva (Palo Alto, CA) and 4-(*N*-hexadecyldimethylammonium)-2,2,6,6-tetramethylpiperidinyloxyl bromide (CAT-16) was from Technika (Sofia, Bulgaria). Heavy water (99.98% ^2H_2O) was purchased from Isotec (Miamisburg, OH). The other chemicals were from Slavus (Bratislava, Slovakia) and were of analytical grade. Organic solvents were redistilled before use.

Sample Preparation

Weighted amounts of EYPC, cholesterol and β-sitosterol were dissolved in chloroform. Required volumes of EYPC and sterol (cholesterol or β-sitosterol) solutions were mixed in glass test tubes. The solvent was evaporated to dryness under a stream of pure gaseous nitrogen, followed by evacuation in a vacuum chamber (≈5 Pa) for 8 h. For small-angle X-ray diffraction (SAXD) measurements, every sample contained about 10 mg of dry lipid (EYPC or EYPC + sterol). The dry lipid was hydrated by approximately 0.1 ml of redistilled water (1 MΩ cm). The test tube was then thoroughly flushed with pure gaseous

nitrogen and sealed with Parafilm M (American National Can, Greenwich, CT). Samples were homogenized by extended vortexing. Before measurements, the suspension was centrifuged and the sediment was filled into a sandwich-type sample holder and used for measurement.

For small-angle neutron scattering (SANS) measurements, the dry lipid (EYPC or EYPC + sterol) was hydrated by heavy water so that lipid concentration was 10 g/l. The test tube was thoroughly flushed with pure gaseous nitrogen and sealed. Samples were homogenized by extended vortexing. Unilamellar vesicles were prepared by dispersion extrusion (Macdonald et al. 1991) through one polycarbonate filter (Nuclepore, Plesanton, CA) with pores of 50 nm diameter, using the LiposoFast Basic extruder (Avestin, Ottawa, Canada) fitted with two gas-tight syringes (Hamilton, Reno, NV). Each sample was subjected to 51 passes through the filters at room temperature. An odd number of passes were performed to avoid contamination of the sample by multi- and oligolamellar vesicles, which might not have passed through the filter. The samples thus prepared were placed into 2-mm quartz cells (Hellma, Müllheim, Germany), closed in nitrogen atmosphere and stored at room temperature. The maximum period between the sample preparation and its measurement was 5 h.

For electron spin resonance (ESR) measurements I, the suspension of multilamellar liposomes was prepared by hydration of dry lipid with aqueous solution of NaCl (150 mmol/l) so that lipid concentration was 25 mg/ml. Spin labels 16-DSA and CAT-16 were dissolved in methanol. Appropriate amounts of these solutions were placed into plastic microtubes, and methanol was evaporated. Suspension of multilamellar liposomes was added to microtubes, and samples were homogenized by vortexing. For ESR measurements II using CSL spin label, weighted amounts of EYPC, sterol and CSL were dissolved in chloroform and required volumes of solutions were mixed in glass test tubes. The solvent was evaporated to dryness under a stream of pure gaseous nitrogen, followed by evacuation in a vacuum chamber. Dry samples were then hydrated by aqueous solution of NaCl (150 mmol/l) so that lipid concentration was 25 mg/ml. Samples were filled into glass capillary tubes (Superior, Marienfeld, Germany) and sealed. The molar ratio of spin label to lipid in all samples was $\leq$0.01.

X-Ray Diffraction

SAXD and wide-angle X-ray diffraction (WAXD) were performed at the soft-condensed matter beam line A2 at HASYLAB DESY (Hamburg, Germany) with monochromatic radiation of wavelength $\lambda = 0.15$ nm. The evacuated double-focusing camera was equipped with two linear delay line readout detectors. The raw data were normalized against the incident beam intensity using the signal of the ionization chamber. The detector for the small-angle region was calibrated by measuring rat tail collagen (Bigi and Roveri 1991), and the detector for the wide-angle region was calibrated by tripalmitin (Chapman 1962). The sample was equilibrated at 25 ± 0.1°C before measurement. Each diffractogram was recorded for 10 s. Diffractograms were plotted as dependences of the diffracted radiation intensity on the scattering vector modulus: $Q = 4\pi\sin\theta/\lambda$, where 2θ is the scattering angle. Each diffraction peak was fitted with a Lorentzian above a linear background. The lamellar repeat distance was evaluated as $d = 2\pi/Q_1$, where Q_1 is the position of the first order reflection.

SANS

SANS measurements were performed on the Yellow Submarine spectrometer located at the extremity of the cold neutron guide N°2 on the Budapest Research Reactor (Budapest Neutron Centre, Hungarian Academy of Sciences, Budapest, Hungary). Experiments were accomplished with a sample to detector distance of 1.3 and 5.6 m and a neutron wavelength of $\lambda = 0.589$ nm. The sample temperature was set and controlled electronically at 25 ± 0.5°C. The data acquisition time for each sample was 30 min.

The normalized SANS intensity, $I_{\exp}(Q)$ (cm^{-1}), was obtained as described in detail (Kučerka et al. 2004b). Examples of SANS data are shown in Fig. 2, together with the best fits as obtained using the so-called 3T model of a bilayer structure (Kučerka et al. 2004b). In particular, the scattering intensity, $I(Q)$, for a polydisperse system of spherical vesicles has the form

$$I(Q) = \int_R G(R) \cdot \left[4\pi \int_{R-d/2}^{R+d/2} r^2 \Delta\rho(r) \frac{\sin(qr)}{qr} \mathrm{d}r \right]^2 \mathrm{d}R \qquad (1)$$

where the distribution of the radii of the unilamellar liposomes, $G(R)$, is assumed to be a Schulz distribution. The scattering length density (SLD), $\rho(r)$, is a function of the radial distance from the center of the unilamellar liposome and $d = d_B$ is the bilayer thickness. $\Delta\rho(r)$ is the difference of SLD between the bilayer and water.

The 3T model (Kučerka et al. 2004b) assumes that the bilayer can be divided into three distinct shells: the nonpolar shell is in the central part of the bilayer (thickness d_{HC}) and two polar headgroup regions (thickness d_H) are in contact with the aqueous phase. The nonpolar central part and the polar headgroup regions are represented by different SLD values. The borders of the headgroup region are not sharp—water molecules from the aqueous phase can

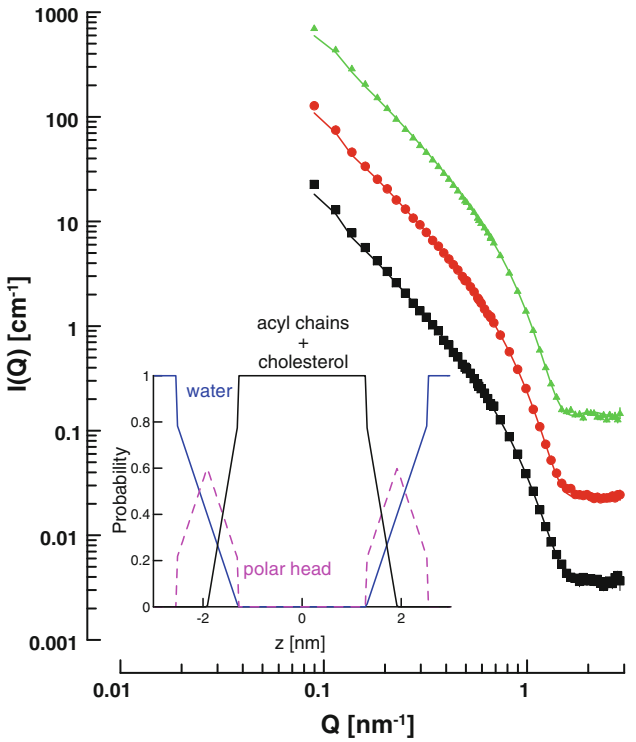

Fig. 2 Experimental SANS data obtained from unilamellar liposomes of EYPC + cholesterol. The content of cholesterol from the bottom is 9.46 mol%, 23.1 mol% and 37.5 mol%. The particular SANS curves are shifted vertically for clarity of presentation. The volume probability distributions of water, polar headgroups, acyl chains and cholesterol are shown in the *inset* as a dependence on the distance from the bilayer center z

penetrate into the headgroup region from the outer side and nonpolar groups from the inner side (Fig. 2 inset). In particular, the probability distribution of water molecules inside the polar region decreases linearly toward the bilayer center according to

$$P_{\mathrm{W}}(r) = -kr + c_2 \tag{2}$$

and the probability distribution of the polar groups (choline, phosphate, glycerol and carbonyl groups) has a triangular shape. Throughout the outer part of the headgroup region, it is then described by the linear function

$$P_{\mathrm{H}}(r) = kr + (1 - c_2) \tag{3}$$

and throughout the inner part of this region by

$$P_{\mathrm{H}}(r) = -kr + (1 - c_2 - c_1) \tag{4}$$

The remaining part is modeled such that the total probability is equal to unity at each point across the entire bilayer. The nonpolar shell consists of lipid hydrocarbon chains and sterol, with no particular partitioning of the corresponding probabilities. The only assumption in this regard is that the overall SLD of the nonpolar shell is constant outside the interfacial region. The coefficients of probability distributions (k, c_1 and c_2) are then directly related to the thicknesses defined above and to the number of water molecules (N_{W}) localized inside the unit cell (unit cell is formed by the phospholipid and a particular fraction of sterol):

$$k = \frac{2N_{\mathrm{W}}V_{\mathrm{W}}}{d_{\mathrm{H}}(V_{\mathrm{H}} + N_{\mathrm{W}}V_{\mathrm{W}})} \tag{5}$$

$$c_1 = -k(2d_{\mathrm{HC}} + d_{\mathrm{H}}) \tag{6}$$

$$c_2 = kd_{\mathrm{HC}} \tag{7}$$

where V_{W} and V_{H} are the volume of a water molecule and that of phospholipid headgroup, respectively. Equations 5–7 are substituted into Eqs. 2–4, which together define our 3T model and are used to calculate the analytical solution of Eq. 1. The resulting expression is then utilized to fit the experimental data. With the assumption about the volumetric data, our analysis can determine three parameters related to bilayer structure (i.e., N_{W}, d_{H} and d_{HC}) and two parameters related to vesicle structure (i.e., radius and its polydispersity) (Kučerka et al. 2004a).

The SANS data, especially those of protonated lipids dispersed in pure D_2O, proved to be most sensitive to one bilayer parameter—its overall thickness d_{B} (Kučerka et al. 2008a). d_{B} is a sum of d_{H} and d_{HC} defined above (i.e., $d_{\mathrm{B}} = 2[d_{\mathrm{H}} + d_{\mathrm{HC}}]$). The number of independent parameters therefore also needs to be reduced to one. This can be easily done through consideration of the lateral area per unit cell (A_{UC}) that correlates all of these thicknesses via the volumetric constraint

$$A_{\mathrm{UC}} = \frac{V_{\mathrm{H}} + N_{\mathrm{W}}V_{\mathrm{W}}}{d_{\mathrm{H}}} = \frac{V_{\mathrm{HC}}}{d_{\mathrm{HC}}} = \frac{V_{\mathrm{H}} + N_{\mathrm{W}}V_{\mathrm{W}} + V_{\mathrm{HC}}}{d_{\mathrm{B}}} \tag{8}$$

V_{HC} in Eq. 8 is the volume of the bilayer hydrocarbon region that includes hydrocarbon chains of one lipid and a particular fraction of sterol. It should be noted that this is different from volume V_{H}, which includes the lipid headgroup only. This choice of parsing is motivated by the fact that the sterol molecule is, for the most part, embedded in the bilayer's hydrocarbon region. The possible inclusion of the sterol headgroup in V_{H} would cause a difference in total headgroup volume smaller than the uncertainty of its determination, which is about 3% (Uhríková et al. 2007; Sun et al. 1994; Tristram-Nagle et al. 2002).

A_{UC} is the area which is occupied at the lipid–water interface (and is exposed to contact with water phase) by a unit cell, i.e., one EYPC molecule + a particular fraction of sterol molecule. All of the above-mentioned parameters of our model are then calculated via Eqs. 2–8 from the single fitting parameter N_{W} and the assumption about the thickness of the headgroup region, $d_{\mathrm{H}} = 1$ nm (Kučerka et al. 2004a) and the molecular volume of the EYPC polar head group ($V_{\mathrm{H}} = 0.331$ nm^3). In addition, the following

volumetric data were used: 633 nm^3 for cholesterol (Greenwood et al. 2006) and 681 nm^3 for beta-sitosterol (Gallová et al. 2008); 0.0223, 0.0270 and 0.0535 nm^3 for methine, methylene and methyl group, respectively (Uhrí-ková et al. 2007); and 0.030 nm^3 for ^2H_2O (Weast 1969). The average carbon number in one acyl chain of EYPC is 17.8, and the average number of double bonds per one chain is 1.2 (Filípek et al. 1993).

ESR Spectroscopy

ESR spectra of spin labels 16-DSA and CAT-16 were measured by an ERS 230 X-band ESR spectrometer (ZWG AdW DDR, Berlin, Germany) using the 100-kHz modulation. Typical instrumental settings were center field 335 mT, microwave power 5 mW, modulation amplitude 0.05 mT, the rate of magnetic field sweep 0.025 mT/s at 0.5 s time constant and sweep width 10 mT. ESR spectra of spin label CSL were measured by a Bruker EMX ESR spectrometer (Karlsruhe, Germany) using the 100-kHz modulation. Typical instrumental settings were center field 335 mT, microwave power 1 mW, modulation amplitude 0.1 mT, the rate of magnetic field sweep 0.1192 mT/s at 0.041 s time constant and sweep width 10 mT. All ESR measurements were carried out at room temperature.

The width of the central line (peak-to-peak distance), $\Delta H(0)$, was evaluated from spectra of 16-DSA. This parameter characterizes the rate of N–O$^\bullet$ fragment motion (Schreier et al. 1978). The distance, A_{max}, between outer extrema (low-field maximum and high-field minimum) was evaluated from the spectra of CSL and CAT-16 spin label. In the case of CSL, this parameter is sensitive to deviation of the long molecular axis of CSL from the normal to bilayer (Lapper et al. 1972).

Results and Discussion

The influence of increasing cholesterol and β-sitosterol concentrations on multilamellar liposomes prepared from EYPC was studied by synchrotron radiation diffraction. We observed two peaks in the small-angle range, whose positions indicated lamellar arrangement. The repeat distance d, representing the sum of water layer thickness d_W and lipid bilayer thickness d_B, was calculated as $d = 2\pi/Q_1$, where Q_1 is the first peak position. In the range of wide angles we found a wide diffuse peak typical for lipids in fluid state. Its position could not be evaluated precisely because of a high noise to signal ratio.

The plot in Fig. 3 shows the repeat distance d in dependence on increasing concentration of sterols in EYPC bilayers. The concentration of sterols is indicated as a mole fraction percentage, $X = 100 \times n_{STEROL}/(n_{STEROL} + n_{EYPC})$, where n_{STEROL} and n_{EYPC} are the number of moles of

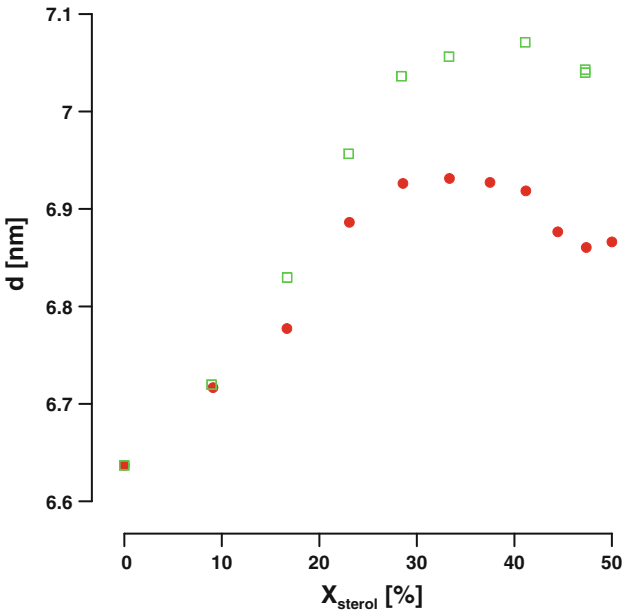

Fig. 3 Dependence of the repeat distance d for the multilamellar liposomes of EYPC on the cholesterol (*filled circle*) or β-sitosterol (*open square*) mole fraction

sterols (cholesterol or β-sitosterol) and EYPC in the sample, respectively. The repeat distance d for EYPC in the absence of sterols is 6.637 ± 0.001 nm, which is consistent with the 6.63 nm reported by Nagle and Tristram-Nagle (2000). As can be seen in Fig. 3, d increases nearly linearly with increasing sterol mole fraction up to about 29 mol%. Above this value of X, d remains almost constant for β-sitosterol and slightly decreases for cholesterol. It is obvious that the presence of β-sitosterol at $X \geq 17$ mol% results in a higher value of d compared to cholesterol. The influence of cholesterol on the repeat distance in EYPC is similar to that in 1-stearoyl-2-oleoyl-*sn*-glycero-3-phosphatidylcholine (SOPC) (Greenwood et al. 2008).

An additional reflection at $Q = 1.79 \pm 0.25$ nm^{-1} (Fig. 4a) is observed in SAXD data when 41.2 mol% of β-sitosterol was present in EYPC multilamellar liposomes. This reflection becomes more visible at 47.4 mol%. Along with that, a peak at $Q = 10.68 \pm 0.25$ nm^{-1} occurs in the wide-angle range (Fig. 4b). McKersie and Thompson (1979) observed several sharp reflections superimposed on a wide peak at 13.66 nm^{-1} when measuring diffractograms of 1,2-dipalmitoyl-*sn*-glycero-3-phosphatidylcholine (DPPC) in the presence of 50 mol% of β-sitosterol in the WAXD range. The positions of sharp peaks were approximately 13.95, 13.07, 12.57 and 10.49 nm^{-1} and the last of the above-mentioned was the most intense one. Those reflections originated from crystalline clusters of β-sitosterol created in the bilayer at concentrations above the solubility limit. By comparison with these results (McKersie and

Thompson 1979), we suggest that the solubility of β-sitosterol is limited also in EYPC bilayers and its crystallization occurs at mole fractions $X_{\text{sitosterol}} \geq 41.7$ mol% in the EYPC bilayer. Due to a low signal to noise ratio in the WAXD region, we can see only the last reflection of those observed by McKersie and Thompson (1979). The above-mentioned facts indicate a "saturation" of the EYPC bilayer by β-sitosterol at $X_{\text{sitosterol}} \approx 41.7$ mol%.

A similar dependence of the repeat distance d on cholesterol concentrations as in Fig. 3 was observed also in multilamellar liposomes from 1,2-dimyristoyl-*sn*-glycero-3-phosphatidylcholine (DMPC) (Petrache et al. 2004).

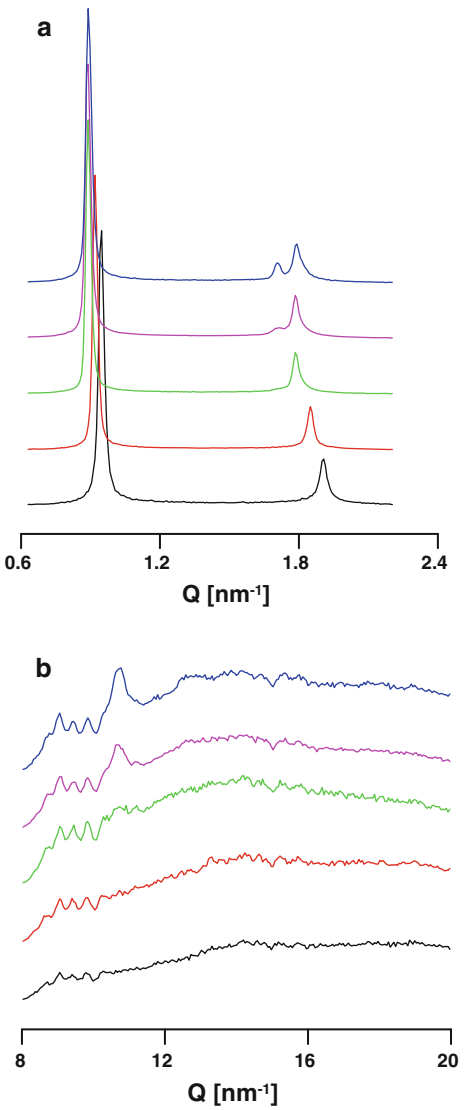

Fig. 4 **a** Difractogram of multilamellar liposomes composed of EYPC + β-sitosterol in the small-angle range. The content of β-sitosterol from the bottom is 0, 23.1, 33.3, 41.2 and 47.4%. **b** Difractogram of multilamellar liposomes composed of EYPC + β-sitosterol in the wide-angle range. The content of β-sitosterol from the bottom is 0, 23.1, 33.3, 41.2 and 47.4%

The change of d from increasing to declining at approximately 26 mol% was explained by a suppression of undulations due to increasing bilayer rigidity (increasing bending modulus) related to a decrease of water layer thickness at cholesterol concentrations of about 26 mol% and above. The L_o state of the bilayer is typical for such cholesterol content in DMPC bilayers. Therefore, our next aim was to investigate the influence of the studied sterols on the lipid bilayer thickness d_B and the water layer thickness d_W.

We performed SANS experiments on unilamelar liposomes made of EYPC and cholesterol or β-sitosterol at 25°C. Only mole fractions of β-sitosterol $X < 40$ mol% were used to avoid crystallization in bilayers. The thickness of lipid bilayer d_B increases approximately linearly with increasing mole fractions of sterols in the entire concentration range (Fig. 5a). A simultaneous fit of both dependences (for cholesterol and β-sitosterol) using the same value of d_B for the sterol-free EYPC bilayer was performed taking into account experimental errors.

In the case of cholesterol, the linear increase of d_B can be characterized as $d_B = (0.014 \pm 0.001) \times X + (4.93 \pm 0.04)$, in nanometers. This is similar to the dependence of d_B on cholesterol mole fractions for 1,2-dioleoyl-*sn*-glycero-3-phosphatidylcholine (DOPC), $d_B = (0.0124 \pm 0.0004) \times X + (4.87 \pm 0.02)$ in nanometers, as obtained in Gallová et al. (2010). The slopes of these two linear dependences are within experimental error the same, suggesting that cholesterol has a similar influence on the thickness of bilayers composed of EYPC or DOPC.

In agreement with these results, the cholesterol-induced increase of fluid phosphatidylcholine bilayer thickness was observed also by other authors for both saturated (Pencer et al. 2005; Hodzic et al. 2008; Pan et al. 2008, 2009) and monounsaturated (Kučerka et al. 2007, 2008b; Hodzic et al. 2008; Pan et al. 2008, 2009; Greenwood et al. 2008; Gallová et al. 2008) chains. The increase of bilayer thickness is related to an increased alignment of the acyl chains in the lipid bilayer, which was proven by the gradual increasing of order parameter detected by 5-DSA spin label at increasing cholesterol concentration (Kusumi et al. 1986; Svorková et al. 2006).

The dependence of d_B on the β-sitosterol molar fraction (Fig. 5a) can be described by the equation $d_B = (0.014 \pm 0.002) \times X + (4.93 \pm 0.04)$, in nanometers. In the range of experimental error, β-sitosterol has a similar effect on the thickness of EYPC bilayers as cholesterol. Comparable ability of cholesterol and β-sitosterol to increase the bilayer thickness of unilamellar vesicles was also observed in our recent reports on DMPC and DPPC bilayers (Gallová et al. 2011) and diCn:1PC (1,2-monounsaturated diacyl-*sn*-glycero-3-phosphatidylcholine with n carbon atoms in the acyl chain) bilayers (n = 14–22)

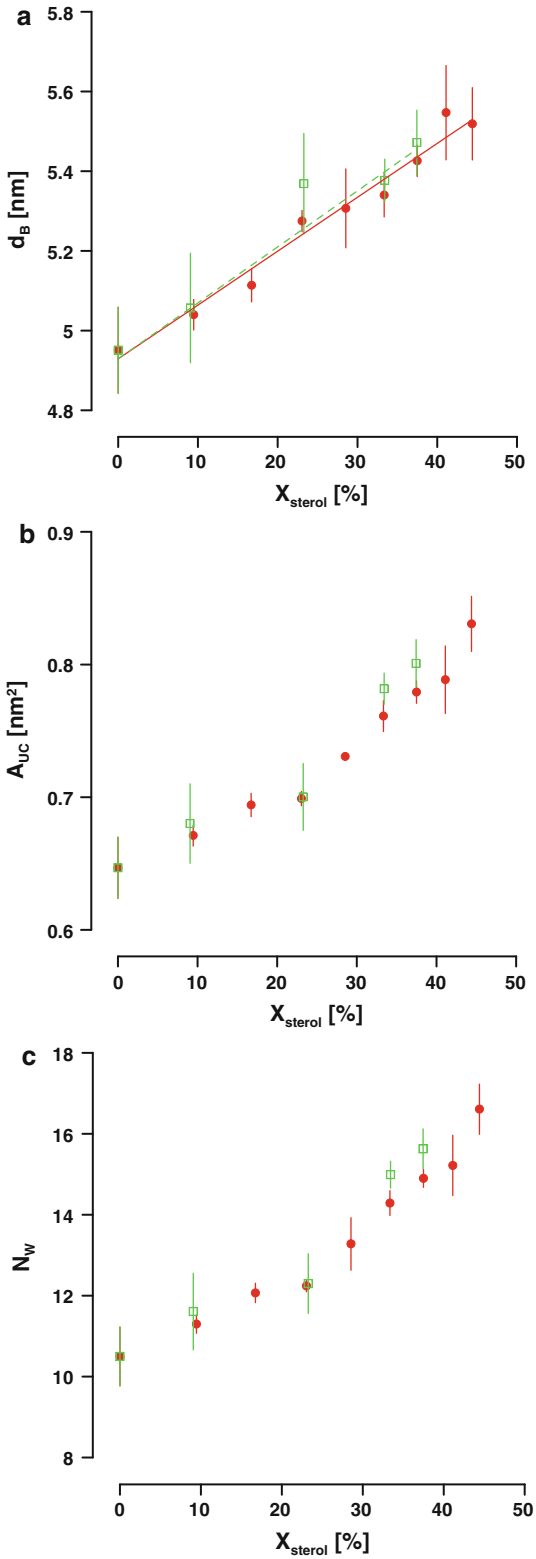

Fig. 5 **a** Dependence of the bilayer thickness d_B on the mole fraction X of cholesterol (*filled circle*) or β-sitosterol (*open square*). **b** Dependence of the unit cell area A_{UC} on the mole fraction X of cholesterol (*filled circle*) or β-sitosterol (*open square*). **c** Dependence of the number of water molecules N_W penetrating into the bilayer polar region on the mole fraction X of cholesterol (*filled circle*) or β-sitosterol (*open square*)

(Gallová et al. 2008). A smaller ability of β-sitosterol in comparison to cholesterol to increase the thickness of hydrated phosphatidylcholine bilayers was reported by other techniques (Hodzic et al. 2008; Krajewski-Bertrand et al. 1992; Bernsdorff and Winter 2003; Hac-Wydro et al. 2007). Such differences between the effects of cholesterol and β-sitosterol on d_B were not observed in our measurements, although the limited accuracy of the SANS method, approximately 0.2 nm for determination of d_B (Fig. 5a), should also be taken into account.

The 3T model used to evaluate our SANS data (Kučerka et al. 2004b) further allows determination of the A_{UC} area, which is occupied at the lipid–water interface by a unit cell, i.e., one EYPC molecule + a particular fraction of sterol molecule, and the number of water molecules N_W associated with this unit cell. It is apparent from Fig. 5b that increasing amounts of both sterols in the EYPC bilayer leads to an increase of A_{UC}. A similar effect of cholesterol on A_{UC} in different phospholipid bilayers was found also by Rog and Pasenkiewicz-Gierula (2006), Kučerka et al. (2007), Greenwood et al. (2008) and Gallová et al. (2008).

The increase of lateral distances between EYPC molecules in the bilayer caused by the intercalation of sterol molecules is accompanied by increased bilayer hydration (Fig. 5c). Because the headgroup region thickness is constrained in the fitting procedure, the number of water molecules N_W penetrating into the bilayer polar region and the A_{UC} parameter are dependent on each other. The shapes of the plots in Fig. 5b and c are therefore identical. The effect of cholesterol and β-sitosterol on headgroup hydration is again similar. In the sterol-free EYPC bilayers, $N_W = 10.5 \pm 0.7$, which is in good agreement with the 10.2 reported by Nagle and Tristram-Nagle (2000).

The knowledge of A_{UC}, the cross-sectional area per unit cell exposed to contact with bulk water phase, at several sterol concentrations allows its partitioning between phospholipid and sterol molecule using the partial molecular area formalism (Edholm and Nagle 2005). Analogous to the concept of partial specific volume that has been employed in physical chemistry (Atkins 1990), partial molecular areas of sterol (a_{STEROL}) and lipid (a_{EYPC}) are defined as

$$a_{STEROL}(X) = \left(\frac{\partial A(X)}{\partial N_{STEROL}}\right)_{N_{EYPC}}$$
$$a_{EYPC}(X) = \left(\frac{\partial A(X)}{\partial N_{EYPC}}\right)_{N_{STEROL}} \quad (9)$$

where $A(X)$ is the total surface of the lipid bilayers in the sample and N_{STEROL} and N_{EYPC} are the numbers of sterol and EYPC molecules in the sample, respectively. Edholm and Nagle (2005) showed that

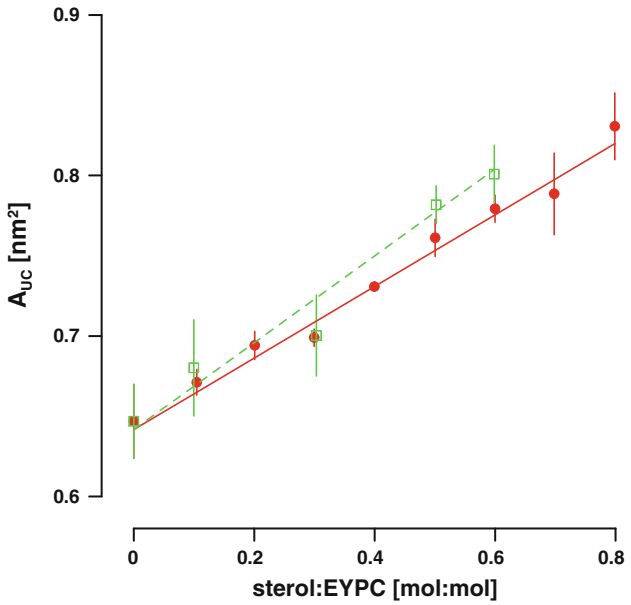

Fig. 6 Dependence of the unit cell area A_{UC} on the molar ratio cholesterol:EYPC (*filled circle*) and β-sitosterol:EYPC (*open square*)

Table 1 Partial molecular areas of cholesterol, β-sitosterol and EYPC

	a_{STEROL} (nm^2)	a_{EYPC} (nm^2)
Cholesterol	0.22 ± 0.02	0.64 ± 0.01
β-Sitosterol	0.27 ± 0.02	0.64 ± 0.01

$$A_{UC}(X) = \frac{A(X)}{N_{EYPC}} = a_{EYPC}(X) + \frac{X}{100 - X} a_{STEROL}(X) \quad (10)$$

where $X/(100 - X)$ is equal to the molar ratio sterol:EYPC. We plotted therefore A_{UC} versus molar ratio in Fig. 6. It is apparent that, within the experimental error, the dependences $A_{UC} = f(X)$ are linear for both cholesterol and β-sitosterol in the studied concentration range. The simultaneous fit of both dependences (for cholesterol and β-sitosterol) using the same value of A_{UC} for the sterol-free EYPC bilayer was performed, taking into account experimental errors. Generally, the partial areas could depend on the molar fraction X (Eq. 9). But once the dependence of $A_{UC}(X)$ on the molar ratio is linear (Fig. 6), a_{EYPC} and a_{STEROL} must be constant, according to Eq. 10. The numerical values of partial areas are shown in Table 1. The physical meaning of partial area per EYPC molecule can be explained as follows. If one molecule of EYPC is added to a sample with a molar ratio sterol:EYPC ≤ 0.8, the resulting increase in total surface of the lipid bilayers in the sample will be equal to $a_{EYPC} = 0.64 \pm 0.01$ nm^2. The same increase in total surface is obtained when one molecule of EYPC is added to a sample composed of sterol-free EYPC bilayers. It can be concluded that partial area per one EYPC molecule in mixed bilayers of cholesterol (or sitosterol) + EYPC is numerically equal to the area occupied by one EYPC molecule at the bilayer–water interface in the sterol-free EYPC bilayer. The value of $a_{EYPC} = 0.64 \pm 0.01$ nm^2 is only a little lower than the value 0.69 nm^2 determined by X-ray diffraction (Nagle and Tristram-Nagle 2000). Moreover, the areas obtained by SANS are systematically smaller than the areas determined by only X-ray diffraction due to differences between the two methods (Kučerka et al. 2008a). Finally, the studied sterols do not decrease the surface occupied by one EYPC molecule at the lipid bilayer–water interface. In other words, these sterols have no condensing effects on the surface occupied by one EYPC molecule.

By measuring the surface tension in a cholesterol monolayer, Hyslop et al. (1990) found that the area per cholesterol molecule was 0.39 nm^2 at 37°C. The partial area $a_{CHOLESTEROL} = 0.22 \pm 0.02$ nm^2 in the EYPC bilayer found in this work is substantially smaller. Again, the physical meaning of partial area per cholesterol molecule can be explained as follows. If one molecule of cholesterol is added to a sample with molar ratio cholesterol:EYPC ≤ 0.8, the resulting increase in total surface of the lipid bilayers in the sample is equal to $a_{CHOLESTEROL} = 0.22 \pm 0.02$ nm^2. A much larger increase in total surface (0.39 nm^2) would be obtained when one molecule of cholesterol is added to a cholesterol monolayer. The facts described above—that (1) the partial area of EYPC in mixed cholesterol + EYPC bilayer is equal to the area occupied by one EYPC molecule in pure EYPC bilayer and (2) the partial area of a cholesterol molecule in mixed cholesterol + EYPC bilayer is smaller than the area occupied by one cholesterol molecule in pure cholesterol monolayer—lead to the following conclusion: From the whole area per cholesterol molecule (0.39 nm^2) only a part of it (0.22 ± 0.02 nm^2) is exposed to contact with aqueous phase in the EYPC bilayer. The rest (0.39 − 0.22 nm^2) is covered by the EYPC polar headgroup. Huang and Feigenson (1999) described this position of cholesterol in phosphatidylcholine bilayer using an "umbrella model." As the hydroxyl group, being the only polar group of cholesterol, covers only a part of the cholesterol surface exposed to water, cholesterol is arranged under phosphatidylcholine polar groups as under an umbrella. As a consequence, the cholesterol molecule reduces the volume occupied by the acyl chains of an EYPC molecule in bilayer. This is why these chains are straightened, the order parameter increases and the bilayer becomes thicker.

Similar values, 0.23–0.26 nm^2, of the partial area of cholesterol as in this work were obtained in our recent study (Gallová et al. 2010) for diCn:1PC (n = 14–22) bilayers using the same experimental and evaluating method.

In contrast to our results obtained for unsaturated phospholipids, the dependence of A_{UC} on the cholesterol:DPPC (Edholm and Nagle 2005) or cholesterol:DMPC (Pan et al. 2009) molar ratio at first decreased, then started to increase at a molar ratio of around 0.1 and only from about 0.5 became approximately linear. As a consequence, a_{CHOL} was negative for molar fractions lower than ≈ 0.15 and increased with increasing X to positive values, stabilizing at 0.27 and 0.37 nm^2 for 50 mol% cholesterol in DPPC and DMPC, respectively. The negative value of a_{CHOL} at low molar fractions is a manifestation of the strong condensing effect of cholesterol on saturated phosphatidylcholines (Edholm and Nagle 2005; Pan et al. 2009). This effect diminishes with increasing cholesterol content.

The concept of partial molecular area was also used in the study of unsaturated phosphatidylcholine DOPC + cholesterol by small-angle X-ray scattering (Pan et al. 2009). The lipid partial area a_{DOPC} decreased from 0.723 nm^2 in the absence of cholesterol to 0.677 nm^2 at 50 mol% of cholesterol. Simultaneously, a_{CHOL} increased from 0.128 nm^2 at 0 mol% of cholesterol to 0.293 nm^2 at 50 mol% of cholesterol. This means that cholesterol displayed a small condensing effect on DOPC, which was much smaller than that on DMPC. The different results in Pan et al. (2009) and in our work could be particularly attributed to the large value of experimental error in our work. This prompted us to employ a simple linear fitting of A_{UC} as a function of molar ratio according to Eq. 10.

The small difference between partial area of β-sitosterol and cholesterol (Fig. 6 and Table 1) could be ascribed to the effect of additional ethyl substituent in the β-sitosterol side chain. However, this subtle difference needs further experimental confirmation.

Figure 3 shows a nonlinear increase of the repeat distance d for EYPC bilayers in the presence of sterols, while Fig. 5a shows a linear increase of the bilayer thickness d_B. Following the above-mentioned facts, the thickness of the interlamellar water layer d_W, separating lipid bilayers in multilamellar liposomes, must also be under the influence of sterols intercalated in the EYPC bilayer. We have determined the water layer thickness as $d_W = d - d_B$ (Fig. 7), where the values of d_B were calculated using the linear dependences of $d_B = f(X)$ stated above. For EYPC in the absence of sterols, the obtained d_W is approximately 1.7 ± 0.1 nm. With increasing cholesterol molar fraction to 33 mol%, d_W slightly decreases, so the increase of d in this concentration range (Fig. 3) is predominantly due to increasing bilayer thickness, caused by cholesterol. With a further increase of cholesterol in the EYPC bilayer, its thickness still increases (Fig. 5a); therefore, the drop of d must be related to a marked decrease of d_W (Fig. 7).

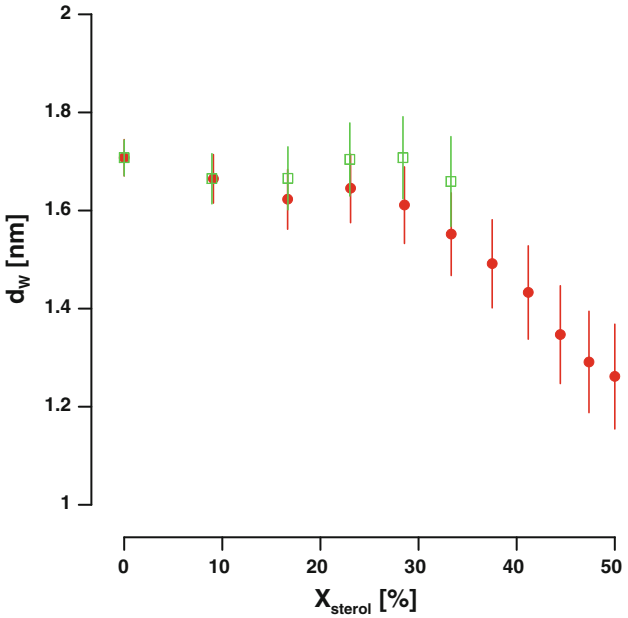

Fig. 7 Dependence of the water layer thickness d_W on the mole fraction X of cholesterol (*filled circle*) or β-sitosterol (*open square*) in EYPC bilayers

The distance between neutral bilayers is determined by a balance of van der Waals attraction forces between single lipid bilayers and repulsive hydration and undulation forces. If the water layer thickness is greater than 1 nm, the hydration forces are negligible and the major effects are due to undulation forces (Petrache et al. 2004). We suppose therefore that the marked decrease of d_W in the presence of more than 33 mol% of cholesterol is connected with a decrease in undulation fluctuations of the bilayer and with an increase in the bending modulus. This can be related to the formation of an L_o state.

More than a fourfold increase of the bending modulus was observed in DMPC + 33.3 mol% of cholesterol compared to neat DMPC above the temperature of the main phase transition (Pan et al. 2008, 2009). In bilayers composed of lipids with one saturated and one unsaturated chain, this effect is smaller but still significant. More than a 1.8-fold increase of the bending modulus was observed in a bilayer from SOPC in the presence of 50 mol% cholesterol (Pan et al. 2008). If the bilayer contained phosphatidylcholine with both monounsaturated chains, the effect of cholesterol on the bending modulus was negligible (Pan et al. 2009).

The water layer thickness does not change within experimental error when β-sitosterol is present in the EYPC bilayer at $X \leq 33$ mol% (Fig. 7). For higher mole fractions, crystallization of β-sitosterol in EYPC bilayers was observed (Fig. 4). This means that β-sitosterol is not miscible with EYPC at mole fractions that could cause a significant drop of d_W. It is therefore not certain whether β-sitosterol can induce the L_o state in EYPC bilayers.

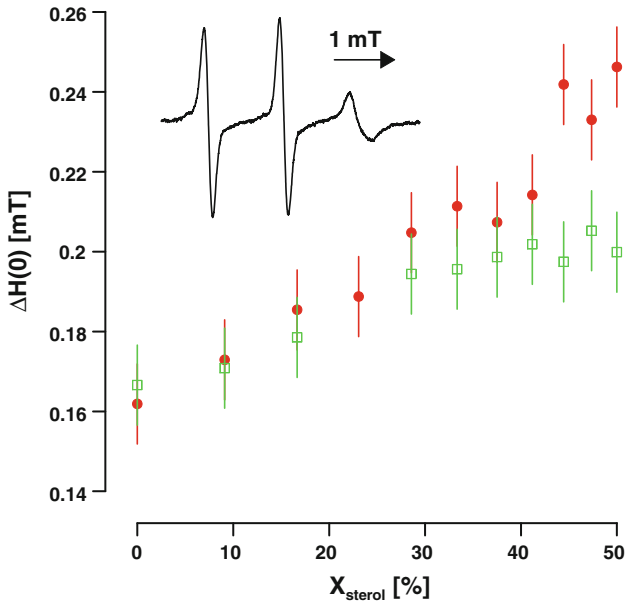

Fig. 8 Dependence of the peak-to-peak width of central line $\Delta H(0)$ on the molar fraction of cholesterol (*filled circle*) or β-sitosterol (*open square*) in EYPC multilamellar liposomes. Spectra were obtained using 16-DSA spin label. *Inset* Spectrum of 16-DSA spin label in EYPC in the absence of sterol

The repeat distance d is higher in the presence of β-sitosterol in EYPC bilayers compared to cholesterol at $X > 17$ mol%. Unfortunately, this difference is near the experimental error of d_W. It is therefore not possible to show unequivocally whether studied sterols in the concentration range $17 \leq X \leq 41$ mol% influence the water layer differently or not. A similar study using saturated phosphatidylcholine DMPC and DPPC showed that both sterols increased the bilayer thickness similarly but cholesterol made the water layer thinner than β-sitosterol (Gallová et al. 2011). A reduction of the multilamellar water layer by sterols was observed also in multilamellar liposomes of POPC (Hodzic et al. 2008) with cholesterol being more effective than β-sitosterol.

We further examined the influence of cholesterol and β-sitosterol on the EYPC bilayers using different nitroxide spin labels. 16-DSA spin label possesses a paramagnetic N–O$^\bullet$ fragment close to the sixteenth carbon atom of the stearic acid chain, so its spectrum is sensitive to changes in the central part of the bilayer. On the other hand, spin labels CAT-16 and CSL inform about the polar headgroup region. It is apparent from the shape of the 16-DSA spectrum (Fig. 8, inset) that the movement of the spin probe N–O$^\bullet$ fragment is nearly isotropic, so the order parameter formalism could not be used. The central line width, $\Delta H(0)$, characterizes the rate of movement of the N–O$^\bullet$ paramagnetic fragment (Kusumi et al. 1986). An increase of $\Delta H(0)$ due to increasing content of cholesterol (Fig. 8) represents a reduced mobility of chains in the central part of EYPC bilayers. This confirms the known ability of cholesterol to reduce the acyl chain *trans-gauche* isomerization in bilayer in its fluid state (Schreier-Muccillo et al. 1973; Vist and Davis 1990; Miao et al. 2002; Mouritsen and Zuckermann 2004). Our results obtained using 16-DSA spin labels are in good compliance with the older work of Kusumi et al. (1986). The influence of cholesterol and β-sitosterol at $X < 41.2\%$ is the same within the experimental error (Fig. 8). For higher mole fractions of β-sitosterol, however, no further enhancement of the line width is observed, as in the case of cholesterol. Based on our findings obtained by X-ray diffraction, we suppose that this is due to crystallization of β-sitosterol in the EYPC bilayers at its high content in the bilayer. 16-DSA molecules are excluded from β-sitosterol crystalline regions, but the mutual spin labels distance is sufficient and $\Delta H(0)$ is not influenced by spin–spin interaction.

The spin probe CAT-16 provides information about the polar part of phospholipid bilayers. Its positive charge at ammonium nitrogen interacts with the negatively charged phosphate group of lipid molecules, while the alkyl chain with 16 carbon atoms penetrates into the hydrophobic part of lipid bilayers (Balgavý et al. 1992). The distance of outer extrema A_{max} could be evaluated only with a large experimental error due to a shallow high-field minimum. Within this experimental error, cholesterol in the concentration range 0–50 mol% has no influence on A_{max} (results not shown). The typical value of A_{max} was 1.1 mT. Our results indicate that increasing the amount of cholesterol in EYPC bilayers has no influence on the behavior of CAT-16 spin probe. It can be explained by an "umbrella model" (Huang and Feigenson 1999), suggesting that the polar groups of phospholipid at the lipid–water interface "shelter" the cholesterol molecule like an umbrella from contact with water. Because the paramagnetic N–O$^\bullet$ group of the CAT-16 spin probe is ejected more to the aqueous environment, it is not influenced by cholesterol.

For further investigation of the influence of cholesterol and β-sitosterol on multilamellar liposomes from EYPC, we used the spin probe CSL, which has a similar structure to cholesterol. However, it has no double bond and the cholesterol hydroxyl group is replaced by a doxyl group bearing the N–O$^\bullet$ fragment. The orientation of CSL in POPC bilayers is the same as the orientation of cholesterol, but CSL is located deeper in the bilayer and shows a greater mobility of the long molecular axis than cholesterol (Scheidt et al. 2003).

It is obvious from Fig. 9 that increasing cholesterol concentrations in EYPC bilayers results in an increase of the A_{max} parameter. Similar effects of cholesterol on the CSL spectra in lipid bilayers were observed in several studies (Lapper et al. 1972; Kusumi et al. 1986; Korstanje et al. 1990). Cholesterol 20 mol% caused an increase of the

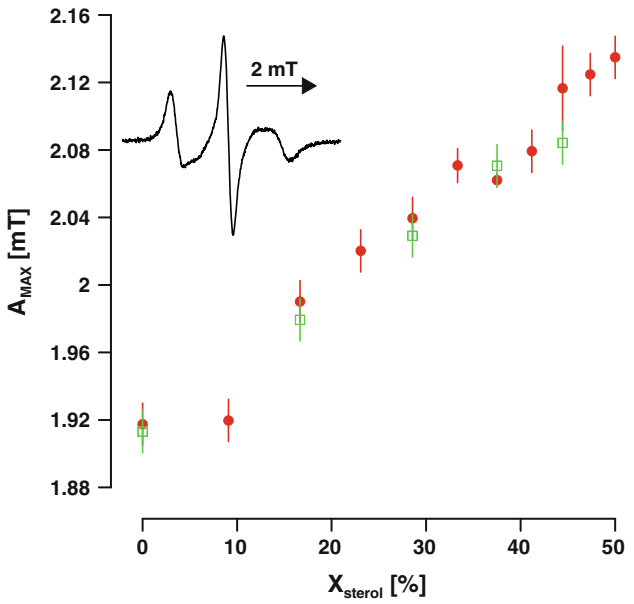

Fig. 9 Dependence of the outer extremum distance A_{MAX} on the molar fraction of cholesterol (*filled circle*) or β-sitosterol (*open square*) in EYPC multilamellar liposomes. Spectra were obtained using CSL spin label. *Inset* Spectrum of CSL spin label in EYPC in the absence of sterol

order parameter for the long molecular axis by 14%, while the diffusion coefficient of rotational motion of the long molecular axis remained constant at 25°C (Korstanje et al. 1990). An increase of the order parameter in the presence of cholesterol in EYPC bilayers was observed also using spin label 5-DSA (Svorková et al. 2006). CSL spectra in EYPC bilayers were measured in the absence of cholesterol and in the presence of 50 mol% cholesterol also at the temperature −120°C in the Q band (Kusumi et al. 1986). The influence of cholesterol resulted in such changes of the values of the main components of the *g*-tensor and of the hyperfine interaction tensor that are typical for increased polarity in the vicinity of the paramagnetic fragment. This was interpreted by an increased penetration of water molecules into the polar region of the EYPC bilayer in the presence of cholesterol. This complies with our results that the number of water molecules in the polar region of the EYPC bilayer increases with increasing cholesterol amount (Fig. 5c).

The paramagnetic fragment N–O$^{\bullet}$ is usually associated with a coordinate system where the *x*-axis is oriented along the N–O bond and *z* is the axis of the 2pπ orbital where the unpaired electron is located. The long molecular axis of CSL is parallel to the *y*-axis. The values of the principal components of hyperfine interaction tensor $A_x \approx A_y$ are five to six times smaller than A_z. At rapid movement of CSL around the long molecular axis in the fluid state of the bilayer, there is an averaging of the A_x and A_z components; and this averaged value is manifested in the CSL spectrum as A_{max}. Kusumi et al. (1986) determined the components of the hyperfine interaction tensor for CSL in DOPC and DOPC + 50 mol% cholesterol bilayers. If we hypothetically suppose a perfectly ordered bilayer (no deviation of the CSL long molecular axis from normal to bilayer) in a fluid state (rapid rotation around the long molecular axis), we could measure $A_{max} = 1.945$ mT in DOPC bilayer and 2.005 mT in DOPC + 50 mol% cholesterol bilayer. The change in A_{max} value (0.06 mT) was ascribed to increased hydration (Kusumi et al. 1986). The increase of A_{max} caused by the addition of 50 mol% cholesterol in our real, not perfectly ordered sample is much higher, approximately 0.218 mT (Fig. 9). We believe that the observed increase of A_{max} is due not only to increased hydration in the polar region but also to increased ordering of the long molecular axis of CSL, similarly as in Korstanje et al. (1990).

It follows from Fig. 9 that the effects of cholesterol and β-sitosterol on the ordering of the long molecular axis of the CSL spin probe are equal within the experimental error.

Finally, we can conclude that β-sitosterol is not miscible with EYPC at $X \geq 41$ mol% as detected by X-ray diffraction and confirmed by ESR spectroscopy using 16-DSA spin label. In the range of full miscibility, the effect of both sterols was similar as observed by spin labels located in the polar or hydrophobic region of bilayers. We found using SANS that in unilamellar vesicles both sterols similarly increase the bilayer thickness and hydration of the headgroup region. The area occupied by sterol and EYPC molecules at the lipid–water interface was determined, but a small, if any, condensing effect of sterols on EYPC interface area was observed. It was demonstrated by SAXD that β-sitosterol at mole fractions $17 \leq X \leq 41$ mol% was more effective at increasing repeat distance than cholesterol. Because of limited experimental precision, we could not show whether it was caused by different effects of the studied sterols on the water layer. Cholesterol in amounts above 33 mol% decreased the interlamellar water layer thickness due to "stiffening" of the bilayer (suppression of undulations). This effect was not manifested by β-sitosterol, in particular due to the fact that β-sitosterol is not soluble in bilayers from EYPC at higher concentrations.

Acknowledgement This work was supported by the European Commission through the Access Activities of the Integrated Infrastructure Initiative for Neutron Scattering and Muon Spectroscopy (NMI3); the European Commission under the 6th Framework Programme through the Key Action: Strengthening the European Research Area, Research Infrastructures, contract RII3-CT-2003-505925; the Dubna JINR 07-04-1069-09/2011 project; and the VEGA 1/0295/08 and 1/0159/11 (P. B.) and 1/0292/09 (D. U.) grants. The research leading to these results has received funding from the European Community's Seventh Framework Programme (FP7/2007-2013) under grant 226716 (HASYLAB project I-20080187 EC, to D. U.).

References

Atkins PW (1990) Physical chemistry, 4th edn. Oxford University Press, Oxford, pp 155–157

Awad AB, Fink CS (2000) Phytosterols as anticancer dietary components: evidence and mechanism of action. J Nutr 130: 2127–2130

Balgavý P, Gallová J, Švajdlenka E, Kutejová E (1992) Probing the membrane polar region with 4-(N-hexadecyldimethylammonium)-2,2,6,6-tetramethylpiperidinyloxyl bromide spin label. Acta Phys Slov 42:228–245

Bernsdorff C, Winter R (2003) Differential properties of the sterols cholesterol, ergosterol, β-sitosterol, trans-7-dehydrocholesterol, stigmasterol and lanosterol on DPPC bilayer order. J Phys Chem B 107:10658–10664

Bigi A, Roveri N (1991) Fibre diffraction: collagen. In: Ebashi S, Koch M, Rubenstein E (eds) Handbook on synchrotron radiation. Elsevier, Amsterdam, pp 199–239

Chapman D (1962) The polymorphism of glycerides. Chem Rev 62:433–453

de Almeida RFM, Fedorov A, Prieto M (2003) Sphingomyelin/phosphatidylcholine/cholesterol phase diagram: boundaries and composition of lipid rafts. Biophys J 85:2406–2416

Edholm O, Nagle JF (2005) Areas of molecules in membranes consisting of mixtures. Biophys J 89:1827–1832

Filípek J, Gelienová K, Kovács P, Balgavý P (1993) Effect of lipid autoperoxidation on the activity of the sarcoplasmic-reticulum (Ca^{2+}–Mg^{2+}) ATPase reconstituted into egg-yolk phosphatidylcholine bilayers. Gen Physiol Biophys 12:55–68

Gallová J, Uhríková D, Kučerka N, Teixeira J, Balgavý P (2008) Hydrophobic thickness, lipid surface area and polar region hydration in monounsaturated diacylphosphatidylcholine bilayers: SANS study of effects of cholesterol and beta-sitosterol in unilamellar vesicles. Biochim Biophys Acta 1778:2627–2632

Gallová J, Uhríková D, Kučerka N, Teixeira J, Balgavý P (2010) Partial area of cholesterol in monounsaturated diacylphosphatidylcholine bilayers. Chem Phys Lipids 163:765–770

Gallová J, Uhríková D, Doktorovová S, Funari SS, Teixeira J, Balgavý P (2011) The influence of cholesterol and β-sitosterol on the structure of saturated diacylphosphatidylcholine bilayers. Eur Biophys J 40:153–163

Gao W, Chen L, Wu F, Yu Z (2008) Liquid ordered phase of binary mixtures containing dipalmitoylphosphatidylcholine and sterols. Acta Phys Chim Sin 24:1149–1154

Greenwood AI, Tristram-Nagle S, Nagle JF (2006) Partial molecular volumes of lipids and cholesterol. Chem Phys Lipids 143:1–10

Greenwood AI, Pan JJ, Mills TT, Nagle JF, Epand RM, Tristram-Nagle S (2008) CRAC motif peptide of the HIV-1 gp41 protein thins SOPC membranes and interacts with cholesterol. Biochim Biophys Acta 1778:1120–1130

Hac-Wydro K, Wydro P, Jagoda A, Kapusta J (2007) The study on the interaction between phytosterols and phospholipids in model membranes. Chem Phys Lipids 150:22–34

Halling KK, Slotte JP (2004) Membrane properties of plant sterols in phospholipid bilayers as determined by differential scanning calorimetry, resonance energy transfer and detergent-induced solubilization. Biochim Biophys Acta 1664:161–171

Hauser H, Poupart G (2009) Lipid structure. In: Yeagle PL (ed) The structure of biological membranes. CRC Press, London, pp 1–52

Hodzic A, Rappolt M, Amenitsch H, Laggner P, Pabst G (2008) Differential modulation of membrane structure and fluctuations by plant sterols and cholesterol. Biophys J 94:3935–3944

Huang JY, Feigenson GW (1999) A microscopic interaction model of maximum solubility of cholesterol in lipid bilayers. Biophys J 76:2142–2157

Hyslop PA, Morel B, Sauerheber RD (1990) Organization and interaction of cholesterol and phosphatidylcholine in model bilayer membranes. Biochemistry 29:1025–1038

Korstanje LJ, Vanginkel G, Levine YK (1990) Effects of steroid molecules on the dynamic structure of dioleoylphosphatidylcholine and digalactosyldiacylglycerol bilayers. Biochim Biophys Acta 1022:155–162

Krajewski-Bertrand MA, Milon A, Hartmann MA (1992) Deuterium-NMR investigation of plant sterol effects on soybean phosphatidylcholine acyl chain ordering. Chem Phys Lipids 63:235–241

Kučerka N, Kiselev MA, Balgavý P (2004a) Determination of bilayer thickness and lipid surface area in unilamellar dimyristoylphosphatidylcholine vesicles from small-angle neutron scattering curves: a comparison of evaluation methods. Eur Biophys J 33:328–334

Kučerka N, Nagle JF, Feller SE, Balgavý P (2004b) Models to analyze small-angle neutron scattering from unilamellar lipid vesicles. Phys Rev E 69:051903

Kučerka N, Pencer J, Nieh MP, Katsaras J (2007) Influence of cholesterol on the bilayer properties of monounsaturated phosphatidylcholine unilamellar vesicles. Eur Phys J E 23:247–254

Kučerka N, Nagle JF, Sachs JN, Feller SE, Pencer J, Jackson A, Katsaras J (2008a) Lipid bilayer structure determined by the simultaneous analysis of neutron and X-ray scattering data. Biophys J 95:2356–2367

Kučerka N, Perlmutter JD, Pan J, Tristram-Nagle S, Katsaras J, Sachs JN (2008b) The effect of cholesterol on short- and long-chain monounsaturated lipid bilayers as determined by molecular dynamics simulations and X-ray scattering. Biophys J 95: 2792–2805

Kusumi A, Subczynski WK, Pasenkiewiczgierula M, Hyde JS, Merkle H (1986) Spin-label studies on phosphatidylcholine-cholesterol membranes—effects of alkyl chain-length and unsaturation in the fluid phase. Biochim Biophys Acta 854: 307–317

Lapper RD, Paterson SJ, Smith IC (1972) A spin label study of the influence of cholesterol on egg lecithin multibilayers. Can J Biochem 50:869–881

Ling WH, Jones PJH (1995) Dietary phytosterols—a review of metabolism, benefits and side-effects. Life Sci 57:195–206

Macdonald RC, Macdonald RI, Menco BPM, Takeshita K, Subbarao NK, Hu LR (1991) Small-volume extrusion apparatus for preparation of large, unilamellar vesicles. Biochim Biophys Acta 1061:297–303

Mateo CR, Acuna AU, Brochon JC (1995) Liquid-crystalline phases of cholesterol lipid bilayers as revealed by the fluorescence of trans-parinaric acid. Biophys J 68:978–987

McKersie BD, Thompson JE (1979) Influence of plant sterols on the phase properties of phospholipid bilayers. Plant Physiol 63:802–805

Miao L, Nielsen M, Thewalt J, Ipsen JH, Bloom M, Zuckermann MJ, Mouritsen OG (2002) From lanosterol to cholesterol: structural evolution and differential effects on lipid bilayers. Biophys J 82:1429–1444

Mouritsen OG, Zuckermann MJ (2004) What's so special about cholesterol? Lipids 39:1101–1113

Nagle JF, Tristram-Nagle S (2000) Structure of lipid bilayers. Biochim Biophys Acta 1469:159–195

Ovesná Z, Vachálková A, Horváthová K (2004) Taraxasterol and beta-sitosterol: new naturally compounds with chemoprotective/chemopreventive effects. Neoplasma 51:407–414

Pan JJ, Mills TT, Tristram-Nagle S, Nagle JF (2008) Cholesterol perturbs lipid bilayers nonuniversally. Phys Rev Lett 100:198103

Pan J, Tristram-Nagle S, Nagle JF (2009) Effect of cholesterol on structural and mechanical properties of membranes depends on

lipid chain saturation. Phys Rev E Stat Nonlinear Soft Matter Phys 80:021931

Pencer J, Nieh MP, Harroun TA, Krueger S, Adams C, Katsaras J (2005) Bilayer thickness and thermal response of dimyristoylphosphatidylcholine unilamellar vesicles containing cholesterol, ergosterol and lanosterol: a small-angle neutron scattering study. Biochim Biophys Acta 1720:84–91

Petrache HI, Harries D, Parsegian VA (2004) Alteration of lipid membrane rigidity by cholesterol and its metabolic precursors. Macromol Symp 219:39–50

Plat J, Mensink RP (2005) Plant stanol and sterol esters in the control of blood cholesterol levels: mechanism and safety aspects. Am J Cardiol 96:15D–22D

Rog T, Pasenkiewicz-Gierula M (2006) Cholesterol effects on a mixed-chain phosphatidylcholine bilayer: a molecular dynamics simulation study. Biochimie 88:449–460

Scheidt HA, Muller P, Herrmann A, Huster D (2003) The potential of fluorescent and spin-labeled steroid analogs to mimic natural cholesterol. J Biol Chem 278:45563–45569

Schreier S, Polnaszek CF, Smith IC (1978) Spin labels in membranes. Problems in practice. Biochim Biophys Acta 515:395–436

Schreier-Muccillo S, Marsh D, Dugas H, Schneider H, Smith ICP (1973) A spin probe study of the influence of cholesterol on motion and orientation of phospholipid in oriented multilayers and vesicles. Chem Phys Lipids 10:11–27

Singleton WS, Gray MS, Brown ML, White JL (1965) Chromatographically homogenous lecithin from egg phospholipids. J Am Oil Soc 42:53–56

Su YL, Li QZ, Chen L, Yu ZW (2007) Condensation effect of cholesterol, stigmasterol, and sitosterol on dipalmitoylphosphatidylcholine in molecular monolayers. Colloids Surf A Physicochem Eng Aspects 293:123–129

Sun WJ, Suter RM, Knewtson MA, Worthington CR, Tristram-Nagle S, Zhang R, Nagle JF (1994) Order and disorder in fully hydrated unoriented bilayers of gel phase dipalmitoylphosphatidylcholine. Phys Rev E 49:4665

Svorková M, Annus J, Gallová J (2006) Effect of cholesterol on the phospholipid bilayers: a spin label study. Acta Facult Pharm Univ Comeniane 53:238–244

Thewalt JL, Bloom M (1992) Phosphatidylcholine–cholesterol phase-diagrams. Biophys J 63:1176–1181

Tristram-Nagle S, Liu Y, Legleiter J, Nagle JF (2002) Lipid bilayers: thermodynamics, structure, fluctuations, and interactions. Biophys J 83:3324

Uhríková D, Rybár P, Hianik T, Balgavý P (2007) Component volumes of unsaturated phosphatidylcholines in fluid bilayers: a densitometric study. Chem Phys Lipids 145:97–105

Veatch SL, Keller SL (2005) Miscibility phase diagrams of giant vesicles containing sphingomyelin. Phys Rev Lett 94:148101

Vist MR, Davis JH (1990) Phase equilibria of cholesterol/dipalmitoylphosphatidylcholine mixtures: ^{2}H nuclear magnetic resonance and differential scanning calorimetry. Biochemistry 29: 451–464

Weast RC (1969) Handbook of chemistry. Chemical Rubber Co., Cleveland, OH